



PRINCIPAL FACTS FOR GRAVITY STATIONS IN THE VICINITY OF COYOTE SPRING VALLEY, NEVADA, WITH INITIAL GRAVITY MODELING RESULTS

by **Geoffrey A. Phelps, E.B. Jewel, V.E. Langenheim and R.C. Jachens**

Open-File Report 00-420

2000

Prepared in cooperation with the Southern Nevada Water Authority

This report is preliminary and has not been reviewed for conformity with U.S. Geological Survey editorial standards or with the North American Stratigraphic Code. Any use of trade, firm, or product names is for descriptive purposes only and does not imply endorsement by the U.S. Government.

**U.S. DEPARTMENT OF THE INTERIOR
U.S. GEOLOGICAL SURVEY**

¹ U.S. Geological Survey, 345 Middlefield Road, Menlo Park, CA

This report is preliminary and has not been reviewed for conformity with U.S. Geological Survey editorial standards or with the North American Stratigraphic Code. Any use of trade, firm, or product names is for descriptive purposes only and does not imply endorsement by the U.S. Government.

U.S. DEPARTMENT OF THE INTERIOR

U.S. GEOLOGICAL SURVEY

¹ U.S. Geological Survey, 345 Middlefield Road, Menlo Park, CA

ABSTRACT

Gravity measurements were made along 5 profiles across parts of the Coyote Spring Valley and vicinity in order to aid in modeling the depth and shapes of the underlying basins and to locate faults concealed beneath the basin fill. Measurements were taken at 200 m (660 ft) spacing along the profiles. Models based on these and existing regional data reveal two north-south-trending basins beneath Coyote Spring Valley that reach maximum depths of greater than 1 km (0.6 mi). A small valley, located just east of Coyote Spring Valley and containing Dead Man Wash, includes a small basin about 500 m (1600 ft) deep that appears to be the southern continuation of the northern basin beneath Coyote Spring Valley. The profile gravity data are further used to identify the locations of possible faults concealed beneath the basin fill.

INTRODUCTION

At the request of the Southern Nevada Water Authority, the U.S. Geological Survey conducted a gravity survey in the Coyote Spring Valley and vicinity, Clark and Lincoln Counties, Nevada, during May, 2000. The purpose of the survey was to help define the shapes of young basins filled with Cenozoic rocks and alluvium, and to identify any possible faults within these basins that might influence the movement of groundwater. The gravity measurements were taken along detailed profiles crossing the southwestern end of Kane Springs Valley, parts of Coyote Spring Valley, and the small valley (located 25 km (15 mi) WNW of Glendale and Moapa, NV) just east of Coyote Spring Valley that contains Dead Man Wash and a section of Pahrangat Wash (fig. 1).

Coyote Spring Valley is a north-south-trending valley about 80 km (50 mi) north of Las Vegas, NV. The valley areas containing the gravity profiles are bounded on the west by the Sheep and Las Vegas Ranges, on the north by the Delamar Mountains, and on the east by the Meadow Valley Mountains. The Arrow Canyon Range projects from the south into the southernmost gravity profiles (figs. 1 and 2).

The valleys in the study area were created by Miocene extension of the crust that formed the basins and ranges that make up most of Nevada today (Stewart, 1980). The ranges

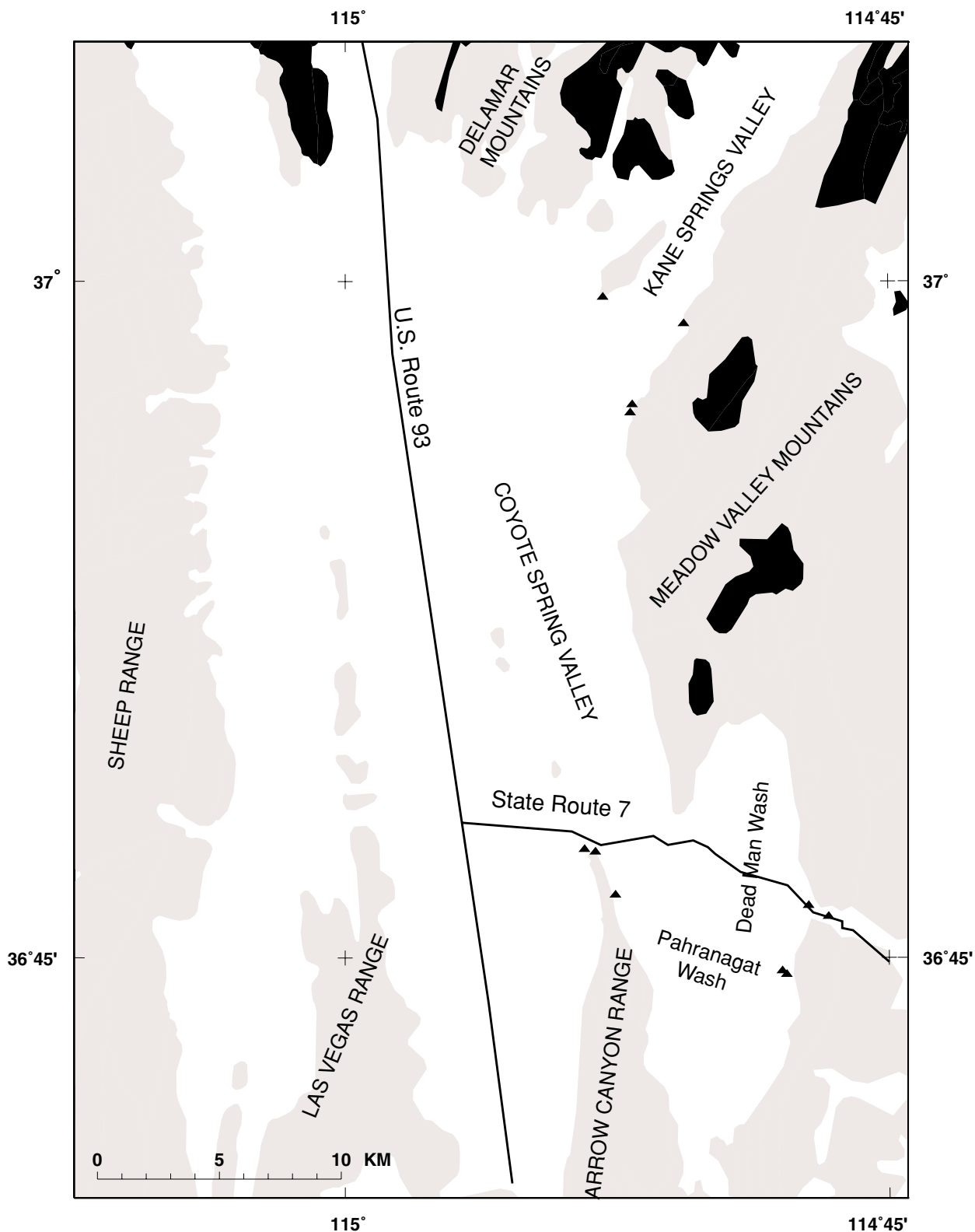


Figure 1. Index map showing Coyote Spring Valley study area and vicinity, Nevada. Black areas have outcrops of Cenozoic volcanic rocks, gray areas have outcrops of Paleozoic rocks, and white areas indicate areas covered by Cenozoic basin fill. Solid triangles indicate locations where samples of Paleozoic rock were collected for density measurements.

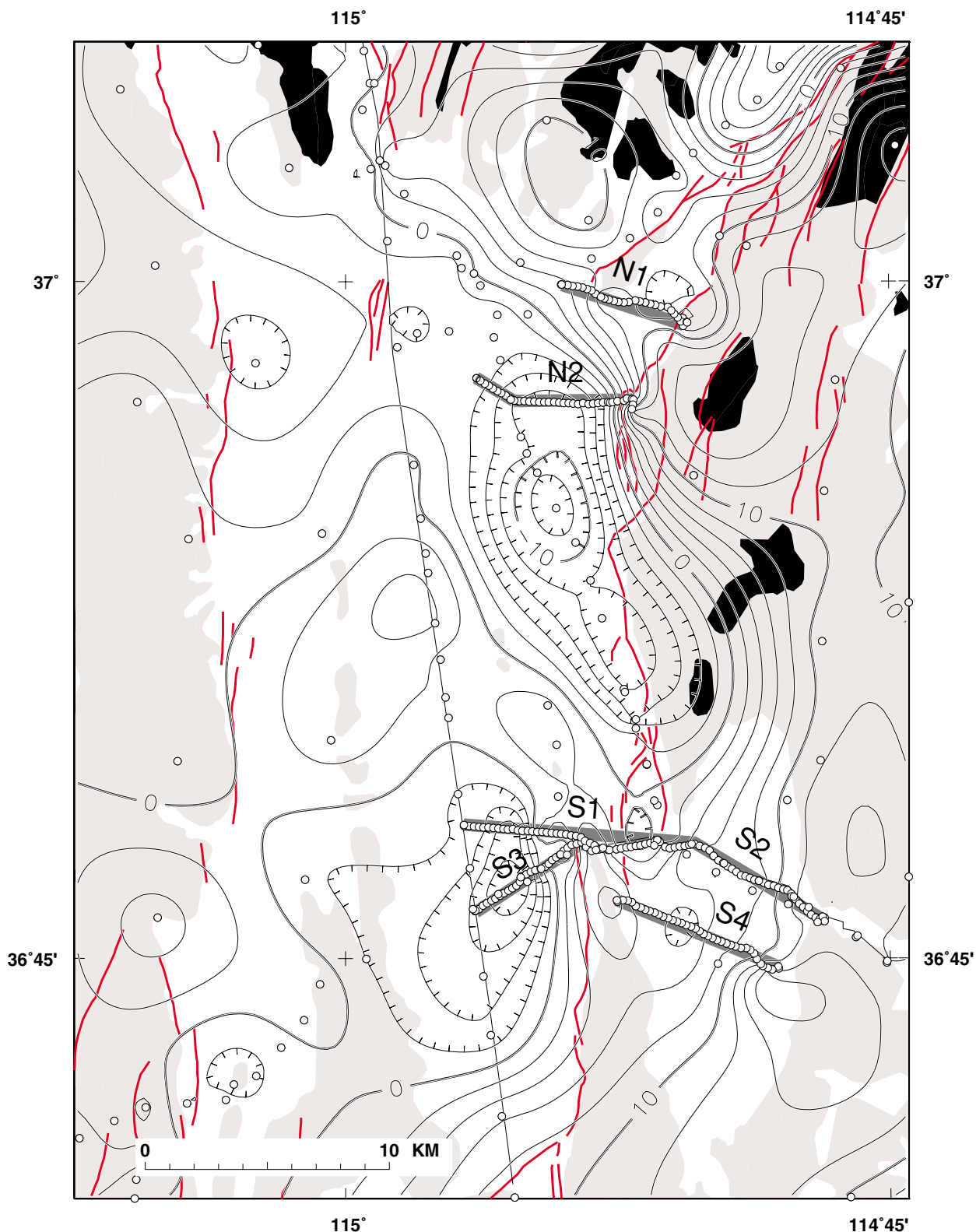


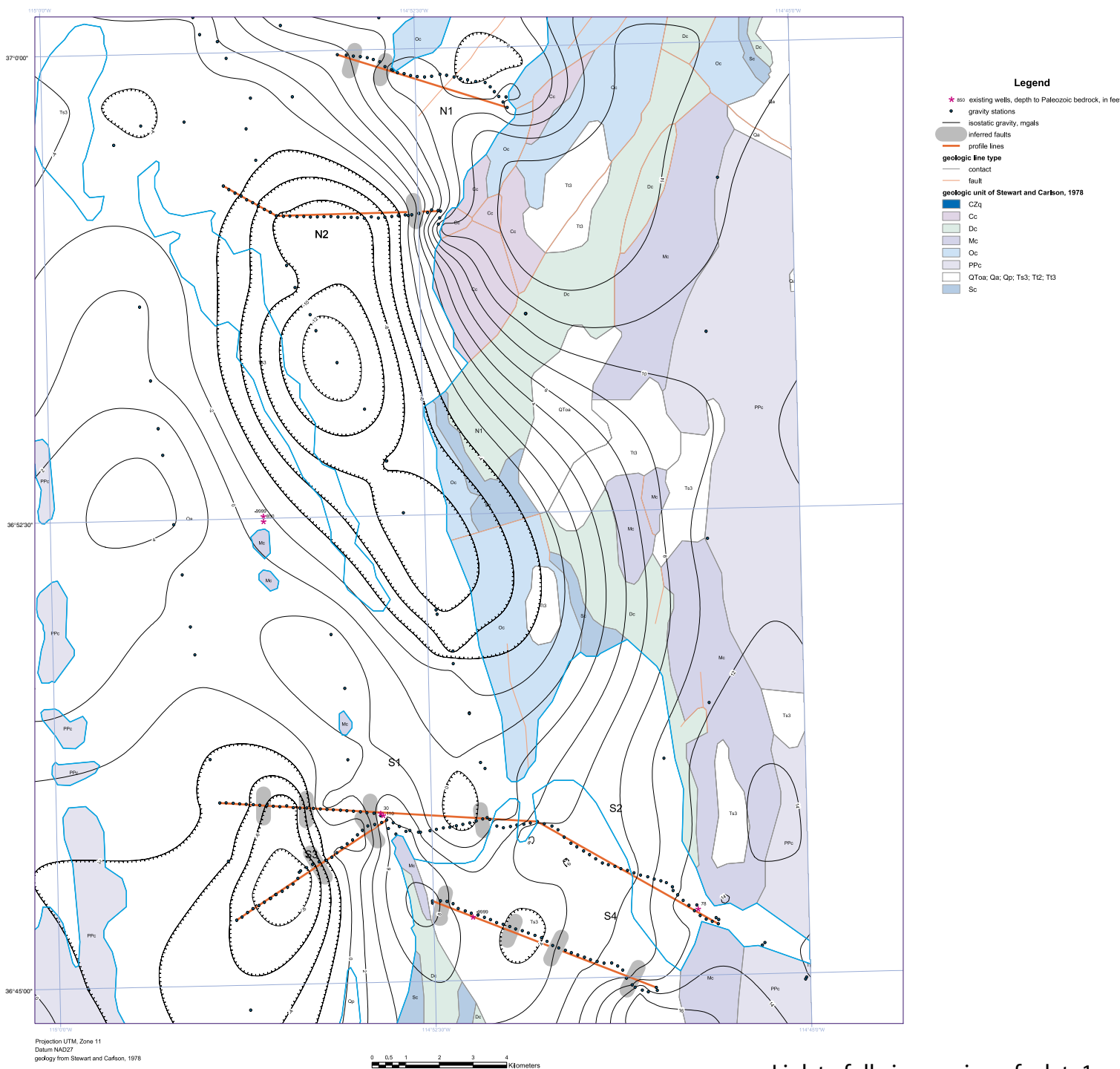
Figure 2. Map showing isostatic residual gravity of Coyote Spring Valley and vicinity. Contour interval = 2 mGal. Open circles show gravity stations. Gray bands labelled N1-N2 and S1-S4 are detailed gravity profiles that were modeled to define basin shape. Red lines indicate faults mapped by Dohrenwend and others (1996). See figure 1 for geology and culture. Refer to Plate 1 for larger scale presentation of these data.

surrounding the study area (and presumably the floors of the intervening basins) are composed primarily of Paleozoic carbonate rocks (Stewart and Carlson, 1978) which typically have densities of 2.7 g/cm^3 or greater. The basins are filled primarily with Miocene tuffaceous sedimentary rocks (with minor tuff) and Quaternary alluvium. These basin fill deposits are typically much lower in density than the Paleozoic carbonate rocks with which they are in contact. Because of the large density contrast between the basin fill and the surrounding carbonate rocks, gravity techniques are well suited for defining the subsurface shapes of the basins and the geometries of the faults that bound the basins.

Previous geophysical work relevant to the present study are limited. Kane and others (1979) and Healey and others (1981) published gravity maps containing about 50 measurements in the vicinity of Coyote Spring Valley. Although more recent compilations more than doubled the number of measurements (Ponce, 1997), the coverage remained too sparse for the purposes of the present study. Geophysical logs for 8 wells in the Coyote Springs Valley area, including 4 wells drilled by the U.S. Air Force as part of the Nevada-Utah MX missile-siting investigation, contain lithologic, density, and electrical information (Berger and others, 1988). Saltus and Jachens (1995) examined the shape and distribution of basins throughout the Basin and Range Province by inverting regional gravity data to yield the thickness of Cenozoic deposits. However, their spatial resolution (2 km) is too coarse to provide useful local information for the present study. Carpenter and Carpenter (1994) analyzed seismic reflection profiles in southern Nevada and surrounding areas, one of which coincides with one of the southern gravity profiles included in this study. This seismic reflection profile provides a valuable check and confirmation of the gravity interpretations.

DATA COLLECTION AND REDUCTION

224 gravity measurements, spaced 200 m (660 ft) apart, were taken along 5 profiles (fig. 2 and plate 1). Measurement locations were determined using a Trimble 1440 RTK (real-time kinematic) Global Positioning System (GPS) to record longitude, latitude, and elevation. Locations were recorded relative to GPS base stations located on local benchmarks. Benchmarks were located horizontally using Rockwell PLGR GPS units, which have an uncertainty of 7 m (23 ft). The vertical datum was provided by the elevation posted on the benchmarks, which gave elevation to the nearest foot. The Trimble RTK System typically has a relative error of 5 to 10 cm (2-4 in) in the horizontal direction and 10-20 cm (4-8 in) in the vertical direction. Therefore, the absolute locations of the gravity observations have uncertainties of at least 7 m (23 ft) horizontally and 0.3 m (1 ft) vertically, but have smaller uncertainties in the relative positions and elevations of data along each profile. The relative positional uncertainties are the important ones for defining the shapes of the basins.



[Link to full-size version of plate1](#)

Isostatic Gravity Anomaly for the Coyote Spring Valley Area

Gravity data were collected during May 2000 using LaCoste and Romberg gravity meter G17c. All gravity data were tied to a gravity base station, GLEN, established at the Glendale Hotel in Glendale, NV. GLEN has a value of 979,682.63 mGal based on ties to LVGS, a gravity base station in front of the U.S. Geological Survey office in Las Vegas, NV (observed gravity 979,593.62 mGal).

Gravity data were reduced using the Geodetic Reference System of 1967 (International Union of Geodesy and Geophysics, 1971) and referenced to the International Gravity Standardization Net 1971 gravity datum (Morelli, 1974, p. 18). Gravity data were reduced to isostatic residual gravity anomalies using standard procedures (e.g. Telford and others, 1976) with a reduction density of 2.67 g/cm^3 and include earth-tide, instrument drift, free-air, latitude, Bouguer, curvature, and terrain corrections. An isostatic correction, using a sea-level crustal thickness of 25 km (16 mi), an upper crustal density of 2.67 g/cm^3 , and a mantle-crust density contrast of 0.40 g/cm^3 , was applied to the gravity data to remove long-wavelength gravity anomalies resulting from isostatic compensation of the topography by deep density distributions. The resulting isostatic residual gravity anomalies reflect, to first order, density variations within the middle and upper crust (Simpson and others, 1986).

Terrain corrections were computed to a radial distance of 167 km (104 mi) and involved a 3-part process: 1) Hayford-Bowie zones A and B with an outer radius of 68 m (223 ft) were estimated in the field with the aid of tables and charts; 2) Hayford-Bowie zones C and D with an outer radius of 590 m (1936 ft) were computed using a 30-m (100-ft digital elevation model; and 3) terrain corrections from a distance of 0.59 km (1936 ft) to 167 km (104 mi) were calculated using a digital elevation model and procedure by Plouff (1977). Total terrain corrections for stations measured during this study range from 0.24 to 3.73 mGal, averaging 1.14 mGal. 95% of the terrain corrections are less than 2 mGal. Uncertainties in the total terrain corrections, based on experience in other areas of Nevada, are estimated to be about 10% of the total correction. Because most of the gravity measurements were made far from the rugged topography that results in large terrain corrections, we estimate the uncertainty in terrain corrections for typical observations in this survey to be less than 0.2 mGal.

The reduced gravity data collected during this study are presented in Appendix 1. We estimate that the total uncertainty associated with these data, based on uncertainties in observed gravity (from meter drift and calibration uncertainties), horizontal position, elevation, and terrain correction, to be typically less than 0.3 mGal, although slightly larger uncertainties correspond to measurements with large terrain corrections (Appendix

1). These uncertainties are substantially smaller than the gravity anomalies associated with the basins, typically on the order of 5.0-10.0 mGal, and do not limit the modeling of the gravity anomalies in terms of basin structure.

The isostatic residual gravity field of the study area, as defined by our new data and all other existing data, is shown in figure 2 and on plate 1. As expected, the valleys are characterized by gravity lows (associated with the low-density deposits contained in them) and the surrounding ranges are characterized by gravity highs.

DENSITY DATA

Sixteen samples were taken at several outcrops (fig. 1) and measurements of sample density were made in the laboratory. With 1 exception the samples are Paleozoic carbonate rocks, which exhibit a mean density of 2.70 g/cm^3 . The density of Quaternary alluvium was not measured directly, but was inferred to be approximately 2.15 g/cm^3 based on density logs in shallow wells within the study area (Berger and others, 1988). Densities of older and deeper basin-filling deposits have not been measured locally within the study area, but have been estimated region-wide (Saltus and Jachens, 1995; Jachens and Moring, 1990), and indirectly measured in a deep well in Mormon Mesa 50 km (30 mi) to the east (Langenheim and others, 2000).

DEPTH TO PALEOZOIC ROCKS

We combined the gravity data collected during this study with existing data to estimate the areal form and distribution of basins in order to provide a regional framework within which to interpret the detailed gravity profiles. We used an iterative gravity inversion method that combines the gravity data with exposed geology, drill hole information, and other geophysical data to estimate the thickness of basin-filling deposits. The method used is an updated version of the method developed by Jachens and Moring (1990) that incorporates additional point data where the basin-fill thickness is known. The method partitions the gravity field into two components, one caused by variations in the thickness of the low-density basin fill, and the other caused by variations of density within the underlying Paleozoic rock. The 'basin-fill' component, together with an assumed vertical variation of density within the basin fill, are inverted to produce a 3-dimensional image of the basins. The method is iterative, successively yielding improved approximations to the shapes of the basins while simultaneously accounting for the gravity field variations caused by density variations within the Paleozoic rock and those caused by the lateral effects of low density basin deposits at locations in the surrounding ranges. For details of this method, the reader is referred to Jachens and Moring (1990) and Saltus and Jachens (1995).

The results of this inversion for Coyote Spring Valley and vicinity are shown in figure 3. The results show two deep basins (the northern crossed by profile N2 and the southern crossed by profiles S1 and S3) beneath the axis of Coyote Spring Valley, both reaching maximum depths greater than about 1 km (3300 ft). The deepest parts of both basins are aligned north-south and are separated from each other by a NNW-trending, shallowly-buried, bedrock ridge that is the northward continuation of the Arrow Canyon Range. A smaller basin (maximum depth of about 500 m (1600 ft)) lies beneath the valley containing Dead Man Wash and part of Pahranaagat Wash, and appears to be the southern continuation of the northern basin beneath Coyote Spring Valley.

The general shapes and locations of the basins are reasonably well constrained by the gravity data, but the details of the basins must be viewed with caution. Except along the detailed gravity profiles, gravity data are sparsely distributed and the resulting basin definition is poor at best. In particular, the southern part of the northernmost basin and the northern part of the Dead Man Wash basin are quite uncertain because of the absence of gravity stations in the Meadow Valley Mountains (fig. 2). A better distribution of gravity stations in the ranges would lead to an improved estimate of the depths of the basins. An interesting characteristic of the southernmost basin beneath Coyote Spring Valley is that the main basin edge (as defined by the abrupt increase in basin depth), does not lie along the western edge of the Arrow Canyon Range, but rather some 2-3 km (1.5-2 mi) west of the range front. The seismic reflection profile analyzed by Carpenter and Carpenter (1994) confirms the offset between the Arrow Canyon Range front and the basin boundary (presumably a normal fault). We do not have enough data to say whether the eastern edge of the northern basin also is systematically displaced westward relative to the range-front of the Meadow Valley Mountains, but the results from gravity modeling discussed in the next section suggest that the basin's edge is within about 1 km (0.6 mi) of the range front.

INTERPRETATION OF DETAILED GRAVITY PROFILES

Gravity models were constructed along 5 profiles (N1-N2 and S1-S4 on figure 2) in order to examine the detailed cross-sectional shapes of the basins and the structures that bound them. A constant density contrast of -0.55 g/cm^3 was used for each model based on a density of 2.70 g/cm^3 for the Paleozoic carbonate rocks and a basin fill density of 2.15 g/cm^3 , the average density of the alluvium measured in two wells near the study area (CSV-1 and CSV-3, in Berger and others, 1988). The results of this modeling are shown in figures 4-6.

Within the Basin and Range province, faults resulting from the Miocene crustal extension often are characterized by abrupt lateral changes in the thickness of Cenozoic basin fill of

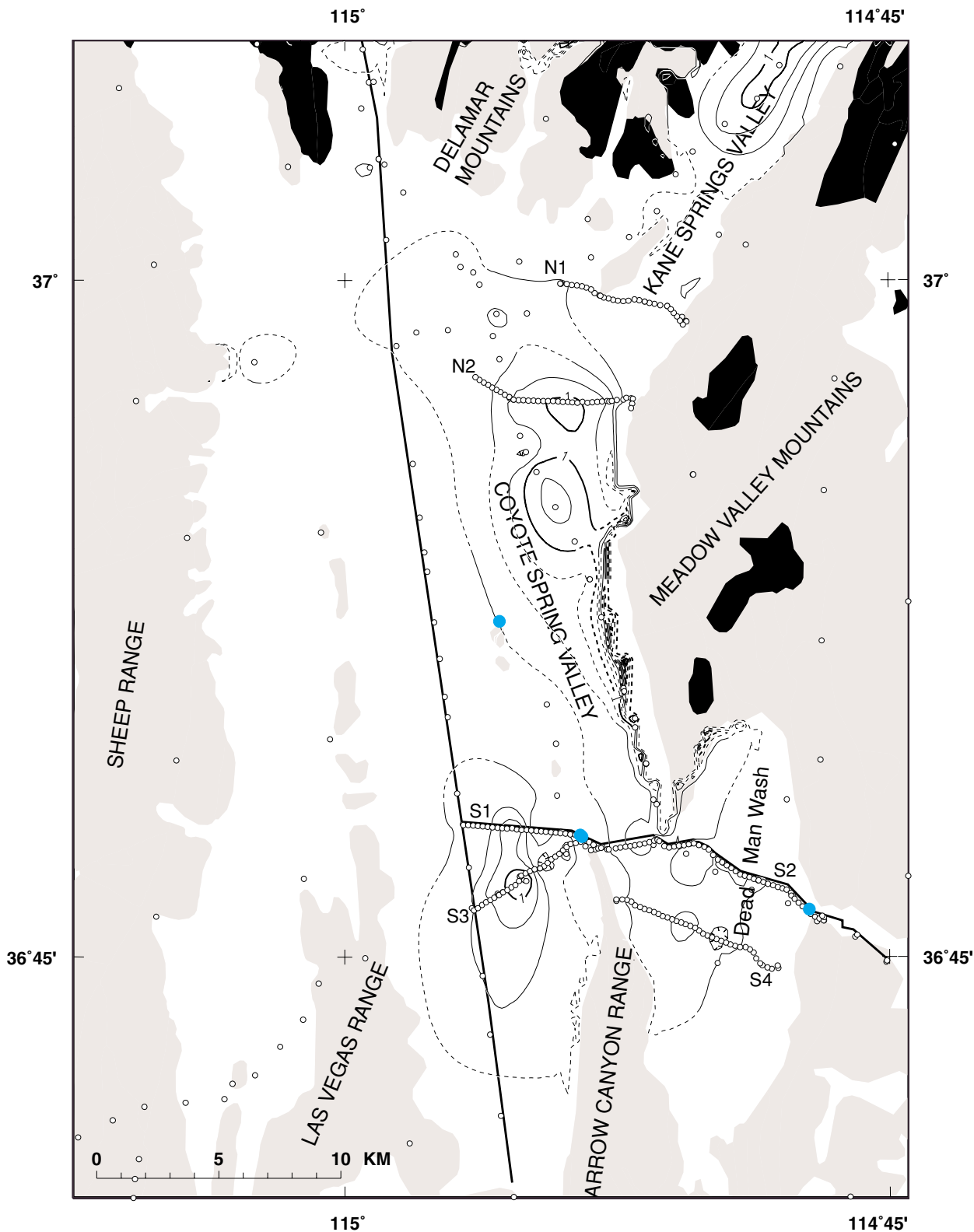


Figure 3. Basin thickness map of the study area. Contour intervals, 250 m, 1 km. Contours dashed where poorly constrained. White and black circles, gravity stations; blue dots, wells that penetrate pre-Cenozoic basement. Black areas have outcrops of Cenozoic volcanic rocks, gray areas have outcrops of Paleozoic rocks, and white areas indicate areas covered by Cenozoic basin fill.

a few hundred meters or more. This relationship is well illustrated along model-profile S1 (fig. 4) where four possible faults are identified in areas of abrupt lateral changes in the thickness of the basin fill. Three of these (identified by asterisks) correspond to faults identified by Carpenter and Carpenter (1994) on the basis of seismic reflection profiling and two (identified by open circles) correspond to faults mapped by Dohrenwend and others (1996). The fourth and westernmost possible fault in figure 4 lies beyond the western end of the seismic reflection profile.

Figure 5 shows gravity models along the two northern profiles, N1 and N2, and figure 6 shows two additional gravity models along southern profiles S3 and S4. Locations of abrupt lateral changes in the thickness of basin fill are identified as possible locations of faults on figures 5 and 6, and their locations in map view are shown on plate 1. A model along profile S2 yielded only a thin, relatively uniform layer of basin fill a few hundred meters thick, and showed no characteristic features that would suggest faults.

The models shown are based on an assumed density contrast of -0.55 g/cm^3 between Paleozoic rock and the basin fill. This density contrast is uncertain primarily because actual measurements of the density of the basin fill are few, and because the density of the fill in the deeper parts of the basin has not been measured locally. We estimate that these uncertainties could be as large as 0.1 g/cm^3 or about 20%. If the actual density contrast along any profile is smaller in magnitude than -0.55 g/cm^3 , the actual depth to Paleozoic rock will be greater than that shown (roughly in proportion to the percentage error). If the actual density contrast is larger, then the depth will decrease. In general, however, the shape of the basin and the locations of abrupt lateral changes in the thickness of the basin fill will not change. Therefore, the locations of possible faults defined by the gravity modeling should not be affected by any reasonable uncertainty in the density contrast used to model the gravity data.

DISCUSSION

Gravity surveys provide an effective method for defining the configuration of concealed Cenozoic basins in the vicinity of Coyote Spring Valley, and, based on a comparison between gravity modeling results and seismic reflection profiling along S1, detailed gravity profiles can be effective in identifying concealed faults. Although the subsurface configuration of the basins are well constrained along the detailed profiles of the present study, the gravity data throughout the rest of Coyote Spring Valley are too sparsely distributed to give more than a generalized image of the basins and their bounding faults. Additional gravity surveys could be used to refine the image of the basins and faults and to trace individual fault strands and establish their continuity. Analysis of aeromagnetic data over the study area in conjunction with the gravity field produced by the Paleozoic

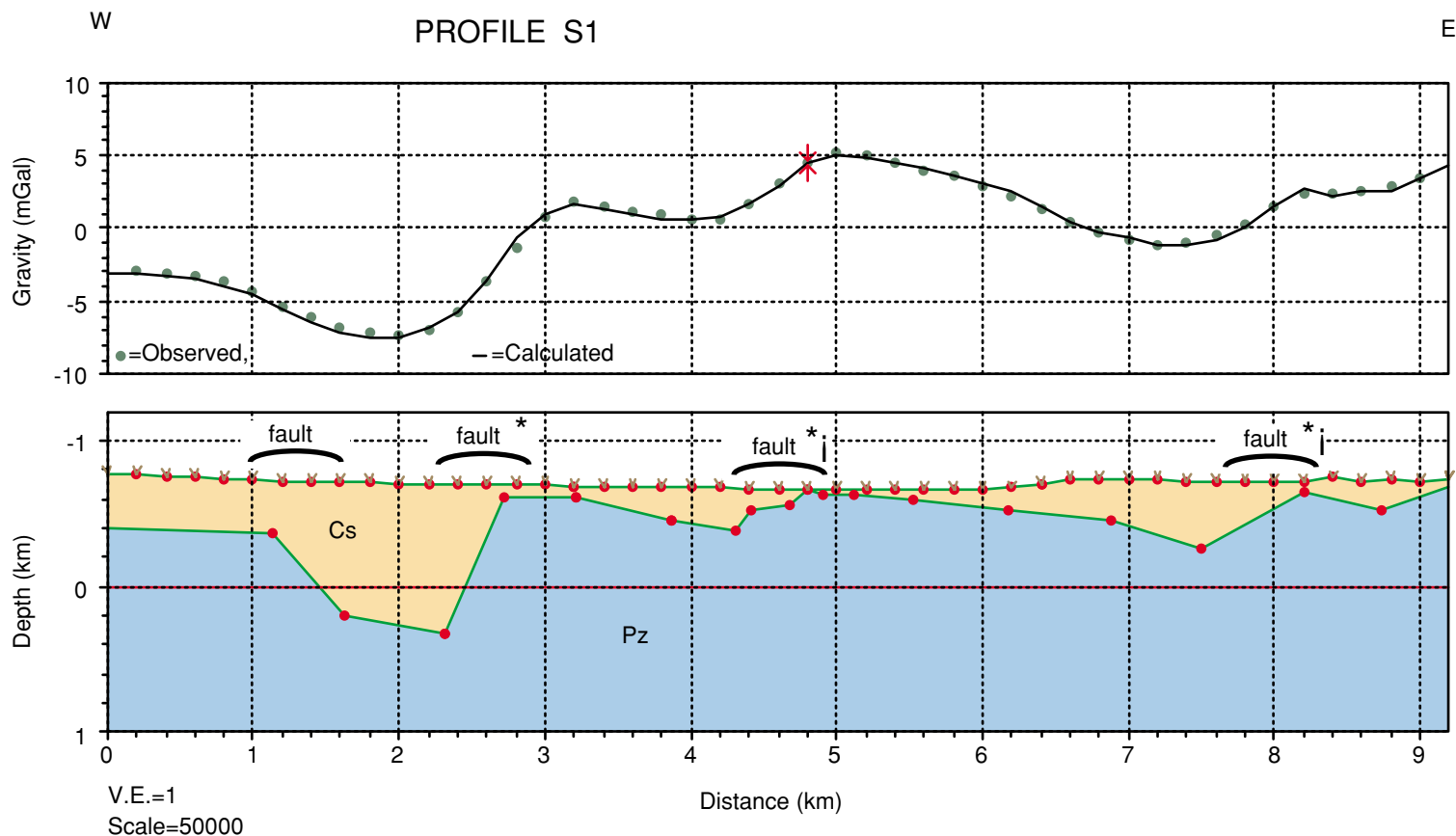


Figure 4. Gravity model along profile S1. Density contrast between Paleozoic bedrock and Cenozoic basin fill, -0.55 g/cm^3 . Pz--Paleozoic rock; Cs--Cenozoic basin fill. Faults marked by asterisks correspond to faults identified by Carpenter and Carpenter (1994) on the basis of seismic reflection profiling and faults marked by open circles correspond to faults mapped by Dohrenwend and others (1996).

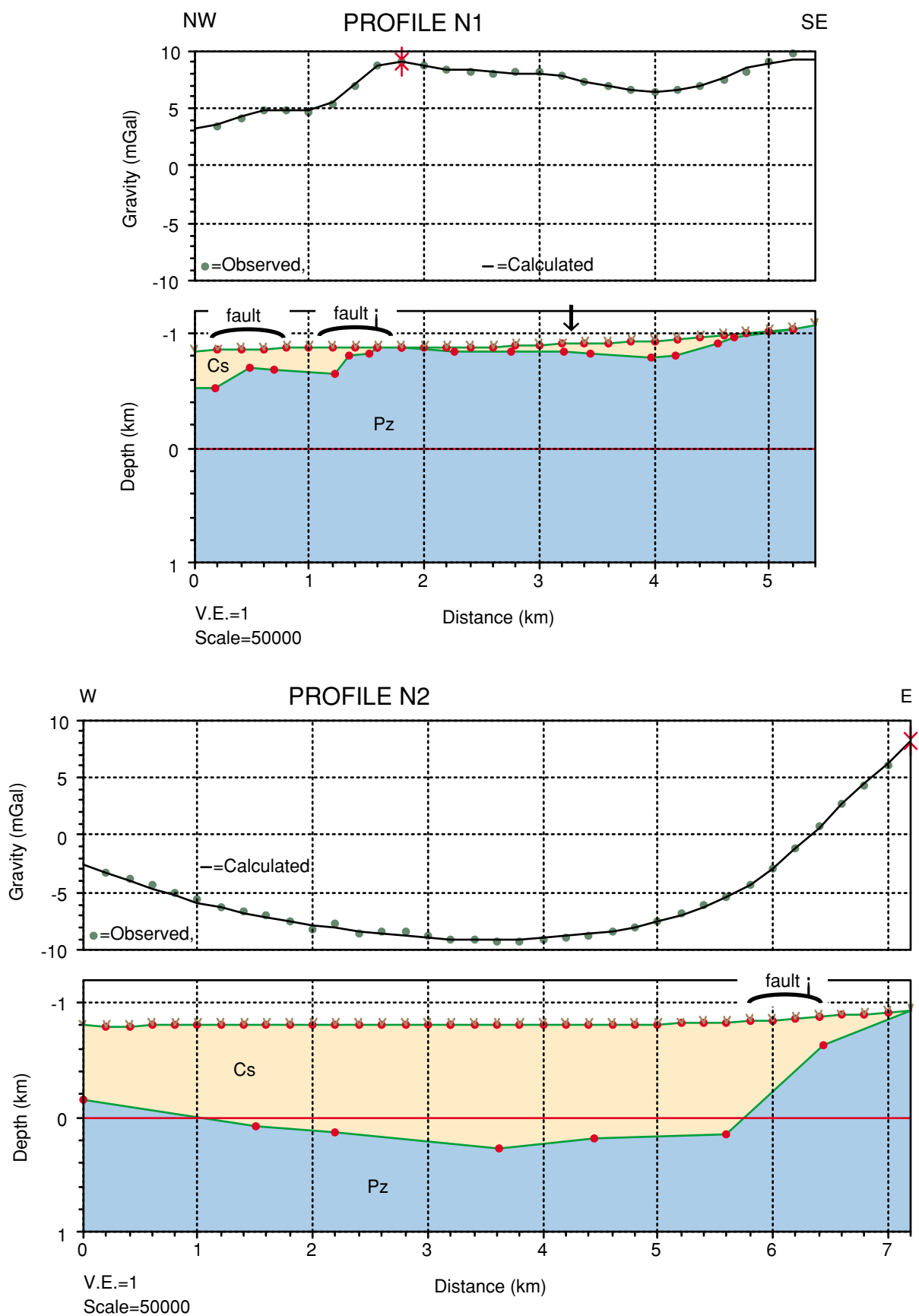


Figure 5. Gravity models along profiles N1 and N2. Density contrast between Paleozoic bedrock and Cenozoic basin fill, -0.55 g/cm^3 . Pz--Paleozoic rock; Cs--Cenozoic basin fill. Faults marked by open circles correspond to faults mapped by Dohrenwend and others (1996). Arrow indicates location of fault shown by Stewart and Carlson, 1978.

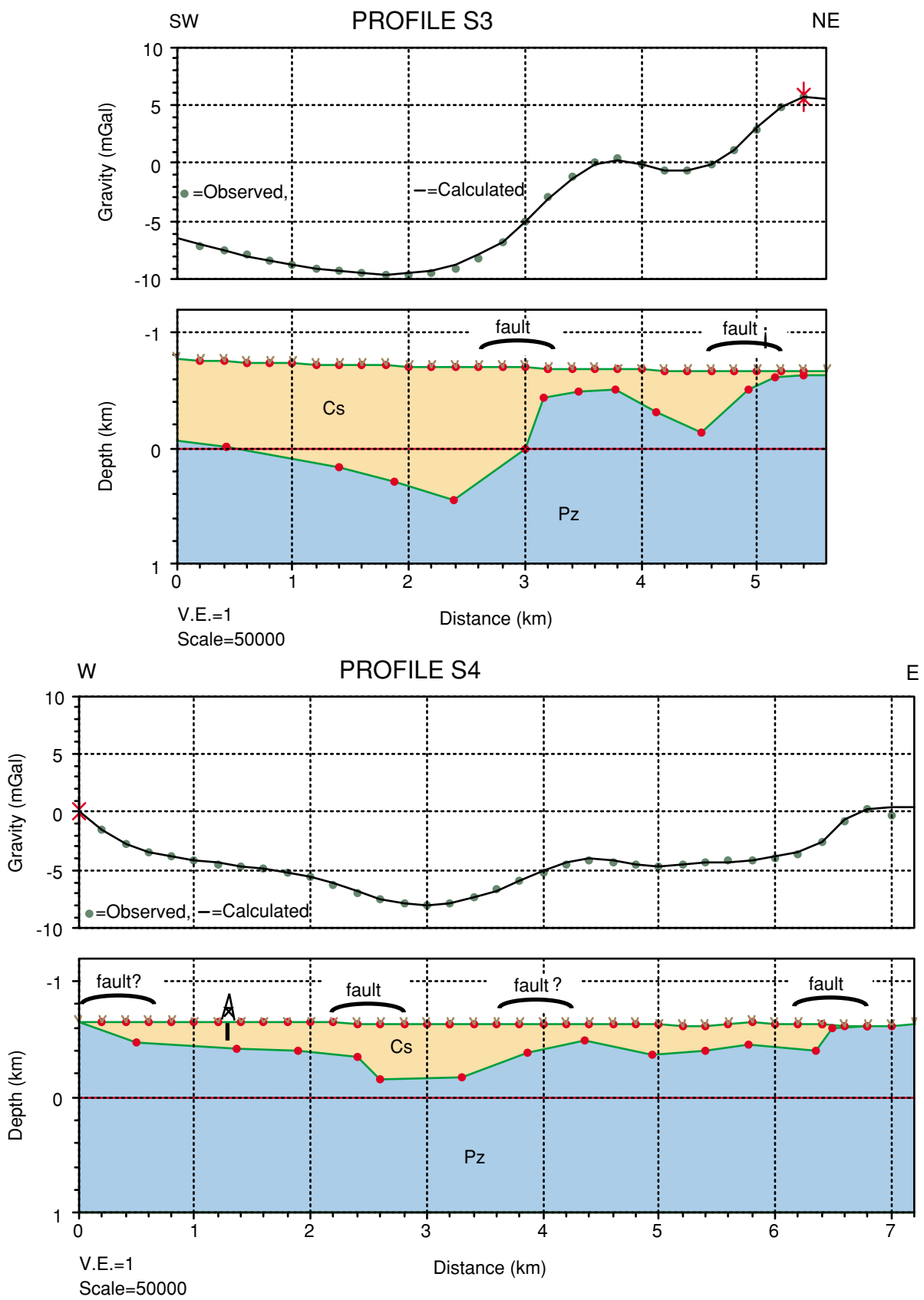


Figure 6. Gravity models along profiles S3 and S4. Density contrast between Paleozoic bedrock and Cenozoic basin fill, -0.55 g/cm^3 . Pz--Paleozoic rock; Cs--Cenozoic basin fill. A linear, westward decreasing regional gradient was removed from profile S4 prior to modeling. Fault marked by an open circle corresponds to a fault mapped by Dohrenwend and others (1996). Well CSV-1 (Berger and others, 1988) is 765 ft deep and did not reach Paleozoic rock.

bedrock (a map that is an outgrowth of the basin-depth inversion) can yield additional information about the lithology and structures within the pre-Cenozoic rock. All of this information could serve as the basis for improving the hydrogeologic framework of the region which, in turn, could be used in a refined ground-water flow model.

REFERENCES CITED

- Berger, D.L., Kilroy, K.C., and Schaefer, D.H., 1988, Geophysical logs and hydrologic data for eight wells in the Coyote Spring Valley area, Clark and Lincoln Counties, Nevada: U.S. Geological Survey Open file Report 87-679, 59 p.
- Carpenter, J.A., and Carpenter, D.G., 1994, Structural and Stratigraphic Relations in a Critical Part of the Mormon Mountains, Nevada, in Dobbs, S.W., and Taylor, W.J., eds., Nevada Petroleum Society 1994 Conference Volume II, (Book 1), p. 95-126.
- Dohrenwend, J.C., Schell, B.A., Menges, C.M., Moring, B.C., and McKittrick, M.A., 1996, Reconnaissance photogeologic map of young (Quaternary and late Tertiary) faults in Nevada: Nevada Bureau of Mines and Geology Open-File Report 96-2.
- Healey, D.L., Snyder, D.B., Wahl, R.R., and Currey, F.E., 1981, Bouguer gravity map of Nevada: Caliente Sheet: Nevada Bureau of Mines and Geology Map 70, scale 1:250,000.
- International Union of Geodesy and Geophysics, 1971, Geodetic Reference System 1967: International Association of Geodesy Special Publication no. 3, 116 p.
- Jachens, R.C., and Moring, B.C., 1990, Maps of the thickness of Cenozoic deposits and the isostatic residual gravity over basement for Nevada: U.S. Geological Survey Open-File Report 90-404, 15 p., 2 plates.
- Kane, M.F., Healey, D.L., Peterson, D.L., Kaufmann, H.E., and Reidy, D., 1979, Bouguer gravity map of Nevada: Las Vegas sheet: Nevada Bureau of Mines and Geology Map 61, scale 1:250,000.
- Langenheim, V.E., Glen, J.M.G., Jachens, R.C., Dixon, G.L., Katzer, T.C., and Morin, R.L., (2000), Gravity and aeromagnetic constraints on the Virgin River Valley depression, Nevada-Utah-Arizona: U.S. Geological Survey Open file Report 00-407.
- Morelli, Carlo, 1974, The International Gravity Standardization Net, 1971: International Association of Geodesy Special Publication no. 4, 194 p.
- Plouff, Donald, 1977, Preliminary documentation for a FORTRAN program to compute gravity terrain corrections based on topography digitized on a geographic grid: U.S. Geological Survey Open-File Report 77-535, 45 p.

Ponce, D.A., 1997, Gravity data of Nevada: U.S. Geological Survey Digital Data Series DDS-42, 27 p., CD-ROM. 80,000 gravity stations.

Saltus, R.W., and Jachens, R.C., 1995, Gravity and basin-depth maps of the Basin and Range Province, western United States: U.S. Geological Survey Geophysical Investigations Map GP-1012, scale 1:2,500,000

Simpson, R.W., Jachens, R.C., Blakely, R.J., and Saltus, R.W., 1986, A new isostatic residual gravity map of the conterminous United States with a discussion on the significance of isostatic residual anomalies: *Journal of Geophysical Research*, v. 91, p. 8348-8372.

Stewart, J.H., 1980, Geology of Nevada: Nevada Bureau of Mines and Geology Special Publication 4, 136 p.

Stewart, J.H., and Carlson, J.E., 1978, Geologic map of Nevada: U.S. Geological Survey, scale 1:500,000

Telford, W.M., Geldart, L.P., Sheriff, R.E., and Keys, D.A., 1976, *Applied Geophysics*: Cambridge University Press, New York, NY, 860 p.

APPENDIX 1: Principal facts for new gravity stations in Coyote Spring Valley and vicinity.

Key to gravity file

Record 1 Station identifier
Record 2 Latitude (in degrees)
Record 3 Latitude (in minutes, to 0.01)
Record 4 Longitude (in degrees)
Record 5 Longitude (in minutes, to 0.01)
Record 6 Elevation (in feet, to 0.1)
Record 7 Observed Gravity (in mGal, to 0.01)
Record 8 Free Air Anomaly (in mGal, to 0.01)
Record 9 Simple Bouguer Anomaly (in mGal, to 0.01)
Record 10 Inner Zone Terrain Correction (in mGal, to 0.01)
Record 11 Total Terrain Correction (in mGal, to 0.01)
Record 12 Complete Bouguer Anomaly (in mGal, to 0.01)
Record 13 Isostatic Residual Anomaly (in mGal, to 0.01)

GLEN	36	3996	114	3409	15030	97968263	-5181	-10307	0	24D	-10342	702
WC001	36	5742	114	5546	26017	97960458	-5178	-14051	6	70D	-14074	-815
WC002	36	5943	114	5110	31515	97958799	-1958	-12707	7	194D	-12620	636
WC002	36	5943	114	5110	31556	97958794	-1925	-12687	7	193D	-12602	654
WC003	36	5919	114	5069	33539	97957767	-1052	-12491	93	373D	-12231	988
WC004	36	5902	114	5067	34375	97957316	-693	-12417	45	355D	-12176	1025
WC005	36	5911	114	5075	33522	97957763	-1061	-12494	36	320D	-12286	925
WC006	36	5920	114	5083	33002	97958009	-1317	-12573	22	273D	-12411	813
WC007	36	5928	114	5092	32424	97958315	-1566	-12624	13	239D	-12495	738
WC008	36	5936	114	5100	31849	97958631	-1802	-12665	10	219D	-12553	693
WC009	36	5945	114	5129	31159	97958995	-2100	-12727	5	163D	-12671	593
WC010	36	5948	114	5145	30819	97959178	-2241	-12752	5	145D	-12713	560
WC011	36	5950	114	5159	30500	97959394	-2328	-12730	4	131D	-12704	577
WC012	36	5953	114	5172	30228	97959637	-2345	-12654	3	121D	-12638	652
WC013	36	5956	114	5187	29920	97959889	-2387	-12591	3	111D	-12584	713
WC014	36	5958	114	5200	29679	97960135	-2370	-12493	3	105D	-12491	812
WC015	36	5955	114	5217	29366	97960349	-2446	-12462	2	100D	-12464	844
WC016	36	5954	114	5231	29126	97960458	-2561	-12495	1	96D	-12501	811
WC017	36	5955	114	5246	28968	97960578	-2591	-12471	1	91D	-12481	837
WC018	36	5957	114	5259	28891	97960631	-2614	-12467	1	87D	-12481	843
WC019	36	5960	114	5272	28797	97960707	-2630	-12452	2	84D	-12468	862
WC020	36	5962	114	5285	28707	97960783	-2642	-12433	3	83D	-12451	886
WC021	36	5967	114	5297	28723	97960857	-2560	-12356	6	82D	-12375	972
WC022	36	5972	114	5310	28568	97960754	-2816	-12560	3	77D	-12583	771
WC023	36	5966	114	5294	28821	97960798	-2526	-12355	6	81D	-12375	969
WC024	36	5980	114	5320	28535	97960575	-3038	-12770	3	75D	-12795	568
WC025	36	5984	114	5333	28763	97960332	-3072	-12882	1	69D	-12914	457
WC026	36	5987	114	5345	28550	97960465	-3144	-12881	4	71D	-12911	467
WC027	36	5989	114	5359	28117	97960764	-3255	-12844	6	74D	-12870	514
WC028	36	5990	114	5373	28011	97960792	-3328	-12881	4	71D	-12910	481
WC029	36	5992	114	5387	27801	97960809	-3511	-12993	3	70D	-13021	376
WC030	36	5993	114	5405	27748	97960793	-3579	-13042	1	66D	-13074	330
WC031	36	4605	114	5644	25062	97960133	-4756	-13304	3	152D	-13243	-636
WC032	36	4610	114	5633	24801	97960249	-4893	-13352	3	150D	-13291	-690
WC033	36	4617	114	5622	24555	97960367	-5016	-13391	2	147D	-13333	-735
WC034	36	4623	114	5611	24316	97960481	-5136	-13429	2	145D	-13372	-780
WC035	36	4628	114	5599	24067	97960602	-5256	-13464	2	144D	-13409	-824
WC036	36	4633	114	5588	23849	97960708	-5362	-13496	2	143D	-13441	-861
WC037	36	4639	114	5576	23661	97960798	-5458	-13528	1	140D	-13474	-900

WC038	36	4645	114	5565	23511	97960894	-5511	-13530	1	137D	-13479	-908
WC039	36	4680	114	5517	23007	97961280	-5650	-13497	4	131D	-13451	-894
WC040	36	4639	114	5575	23657	97960801	-5458	-13527	1	140D	-13474	-901
WC041	36	4645	114	5564	23499	97960900	-5517	-13531	2	138D	-13479	-909
WC042	36	4650	114	5552	23419	97960940	-5559	-13547	1	133D	-13500	-936
WC043	36	4656	114	5541	23241	97961051	-5624	-13551	3	135D	-13502	-942
WC044	36	4661	114	5530	23119	97961146	-5651	-13536	1	131D	-13490	-933
WC045	36	4670	114	5520	23107	97961187	-5634	-13515	1	127D	-13474	-920
WC046	36	4682	114	5514	22972	97961320	-5646	-13481	3	129D	-13436	-880
WC047	36	4687	114	5502	22837	97961496	-5604	-13393	21	148D	-13329	-778
WC048	36	4692	114	5490	22689	97961722	-5524	-13263	8	135D	-13212	-666
WC049	36	4696	114	5477	22573	97962004	-5357	-13056	8	134D	-13005	-468
WC050	36	4698	114	5463	22436	97962349	-5144	-12796	5	132D	-12747	-219
WC051	36	4703	114	5451	22331	97962587	-5012	-12628	16	143D	-12568	-47
WC052	36	4710	114	5441	22228	97962756	-4950	-12531	18	145D	-12469	50
WC053	36	4718	114	5431	22145	97962805	-4990	-12543	17	143D	-12483	32
WC054	36	4724	114	5420	22055	97962829	-5060	-12582	4	128D	-12535	-25
WC055	36	4730	114	5409	22014	97962835	-5101	-12609	3	125D	-12566	-61
WC056	36	4738	114	5399	21939	97962899	-5119	-12602	2	123D	-12560	-59
WC057	36	4745	114	5389	21866	97963000	-5097	-12554	2	121D	-12515	-14
WC058	36	4752	114	5378	21785	97963159	-5024	-12454	3	120D	-12415	83
WC059	36	4754	114	5364	21764	97963408	-4798	-12221	4	118D	-12183	309
WC060	36	4757	114	5350	21663	97963714	-4591	-11979	8	123D	-11938	547
WC061	36	4747	114	5337	21737	97963758	-4463	-11877	25	138D	-11820	651
WC062	36	4738	114	5322	21641	97963836	-4462	-11843	39	156D	-11768	687
WC063	36	4698	114	5462	22434	97962354	-5141	-12792	5	132D	-12744	-217
WC064	36	4794	114	5673	25295	97960544	-4399	-13026	2	137D	-12981	-254
WC065	36	4794	114	5660	25047	97960674	-4502	-13045	3	136D	-13000	-282
WC066	36	4793	114	5646	24795	97960808	-4604	-13061	4	135D	-13016	-307
WC067	36	4792	114	5633	24537	97960951	-4702	-13071	3	133D	-13027	-327
WC068	36	4791	114	5620	24291	97961076	-4807	-13092	3	132D	-13048	-356
WC069	36	4790	114	5606	24060	97961144	-4955	-13161	3	130D	-13118	-437
WC070	36	4789	114	5593	23846	97961184	-5115	-13248	3	129D	-13206	-535
WC071	36	4788	114	5579	23643	97961241	-5247	-13311	2	127D	-13271	-610
WC072	36	4787	114	5566	23460	97961296	-5363	-13364	2	126D	-13325	-673
WC073	36	4786	114	5553	23289	97961371	-5447	-13390	2	124D	-13351	-708
WC074	36	4787	114	5539	23176	97961446	-5480	-13384	11	130D	-13339	-705
WC075	36	4784	114	5526	22999	97961612	-5476	-13320	1	120D	-13284	-662
WC076	36	4783	114	5513	22954	97961772	-5357	-13185	0	116D	-13154	-542
WC077	36	4783	114	5499	22867	97962057	-5153	-12953	15	128D	-12909	-306
WC078	36	4782	114	5486	22791	97962325	-4955	-12729	21	132D	-12680	-87
WC079	36	4781	114	5472	22729	97962581	-4756	-12508	21	130D	-12463	120
WC080	36	4780	114	5459	22661	97962747	-4653	-12382	21	128D	-12338	235
WC081	36	4779	114	5446	22626	97962716	-4715	-12432	4	108D	-12407	156
WC082	36	4778	114	5432	22608	97962698	-4749	-12459	9	111D	-12432	121
WC083	36	4777	114	5419	22535	97962732	-4782	-12468	9	110D	-12442	102
WC084	36	4776	114	5406	22366	97962817	-4854	-12483	2	104D	-12462	73
WC085	36	4775	114	5392	22191	97962936	-4899	-12467	4	107D	-12442	82
WC086	36	4773	114	5379	21978	97963182	-4850	-12346	11	118D	-12310	203
WC087	36	4772	114	5365	21862	97963433	-4707	-12163	9	116D	-12128	374
WC088	36	4768	114	5352	21759	97963609	-4622	-12043	12	121D	-12003	490
WC089	36	4761	114	5340	21691	97963750	-4534	-11932	17	128D	-11886	595
WC090	36	4756	114	5327	21624	97963795	-4545	-11920	11	124D	-11877	594
WC091	36	4750	114	5315	21585	97963801	-4567	-11929	11	125D	-11885	573
WC092	36	4742	114	5302	21537	97963838	-4564	-11909	3	119D	-11871	574
WC093	36	4743	114	5294	21620	97963757	-4568	-11942	21	133D	-11890	551
WC094	36	4740	114	5277	21972	97963484	-4507	-12001	27	126D	-11956	471

WC095	36	5742	114	5546	26243	97960464	-4959	-13910	1	63D	-13941	-683
WC096	36	5736	114	5534	26297	97960380	-4984	-13953	0	62D	-13985	-738
WC097	36	5735	114	5520	26247	97960293	-5116	-14068	1	63D	-14099	-859
WC098	36	5735	114	5507	26265	97960337	-5055	-14013	0	63D	-14045	-810
WC099	36	5734	114	5493	26240	97960334	-5080	-14030	0	64D	-14060	-832
WC100	36	5734	114	5479	26248	97960304	-5103	-14055	0	65D	-14084	-862
WC101	36	5733	114	5466	26354	97960220	-5086	-14074	0	65D	-14103	-888
WC102	36	5733	114	5452	26369	97960203	-5089	-14082	0	67D	-14110	-901
WC103	36	5733	114	5439	26358	97960208	-5094	-14084	0	69D	-14110	-906
WC104	36	5733	114	5425	26519	97960112	-5039	-14083	1	70D	-14108	-912
WC105	36	5732	114	5411	26418	97960199	-5045	-14055	0	73D	-14077	-888
WC106	36	5731	114	5398	26445	97960188	-5029	-14049	0	76D	-14067	-885
WC107	36	5731	114	5384	26525	97960162	-4980	-14027	1	80D	-14042	-865
WC108	36	5730	114	5372	26554	97960162	-4951	-14008	0	82D	-14021	-849
WC109	36	5729	114	5358	26593	97960180	-4895	-13965	0	87D	-13973	-805
WC110	36	5731	114	5344	26610	97960240	-4822	-13898	0	94D	-13899	-736
WC111	36	5729	114	5330	26616	97960300	-4754	-13831	1	103D	-13824	-669
WC112	36	5730	114	5317	26799	97960253	-4630	-13770	2	107D	-13758	-608
WC113	36	5731	114	5303	27099	97960160	-4442	-13685	3	112D	-13669	-524
WC114	36	5732	114	5290	27415	97960076	-4231	-13581	4	117D	-13561	-420
WC115	36	5733	114	5276	27810	97959982	-3955	-13440	8	127D	-13411	-275
WC116	36	5732	114	5270	27982	97959929	-3845	-13388	8	131D	-13356	-223
WC117	36	5733	114	5263	28199	97959903	-3668	-13286	8	135D	-13250	-119
WC118	36	5735	114	5249	28629	97959854	-3316	-13080	7	144D	-13037	91
WC119	36	5736	114	5231	29181	97959779	-2873	-12826	8	163D	-12764	355
WC120	36	5740	114	5223	29390	97959681	-2780	-12804	10	173D	-12733	387
WC121	36	5739	114	5210	29929	97959753	-2200	-12408	23	199D	-12313	800
WC122	36	5738	114	5205	29959	97959569	-2354	-12572	55	240D	-12436	674
WC123	36	5727	114	5207	29873	97959634	-2354	-12543	96	283D	-12364	737
WC124	36	5717	114	5210	30322	97959717	-1835	-12176	99	273D	-12008	1087
WC130	36	4740	114	5273	22244	97963219	-4515	-12102	32	124D	-12061	363
WC131	36	4742	114	5254	22598	97962923	-4481	-12188	32	115D	-12157	255
WC132	36	4744	114	5241	22792	97962738	-4487	-12260	27	105D	-12239	165
WC133	36	4746	114	5227	22951	97962576	-4502	-12330	33	107D	-12307	88
WC134	36	4747	114	5214	23115	97962424	-4501	-12385	32	103D	-12367	19
WC135	36	4749	114	5201	23273	97962299	-4481	-12418	28	96D	-12408	-29
WC136	36	4751	114	5188	23430	97962189	-4446	-12437	26	91D	-12432	-61
WC137	36	4753	114	5174	23520	97962163	-4390	-12412	25	87D	-12411	-47
WC138	36	4756	114	5161	23548	97962199	-4332	-12363	26	87D	-12363	-6
WC139	36	4759	114	5148	23377	97962433	-4263	-12236	15	77D	-12245	104
WC140	36	4761	114	5139	23490	97962460	-4133	-12144	8	68D	-12162	182
WC141	36	4758	114	5134	23359	97962578	-4134	-12101	16	78D	-12109	230
WC142	36	4747	114	5120	23509	97962500	-4055	-12073	30	89D	-12070	249
WC143	36	4744	114	5107	23425	97962587	-4042	-12032	12	71D	-12047	261
WC144	36	4746	114	5093	23328	97962721	-4002	-11959	10	69D	-11975	325
WC145	36	4748	114	5080	23384	97962739	-3935	-11910	7	65D	-11931	363
WC146	36	4749	114	5066	23678	97962604	-3795	-11870	4	59D	-11898	390
WC147	36	4751	114	5053	23782	97962638	-3666	-11777	4	59D	-11805	478
WC148	36	4753	114	5039	23834	97962712	-3546	-11675	4	58D	-11704	574
WC149	36	4749	114	5025	23524	97962925	-3618	-11642	19	74D	-11654	611
WC150	36	4745	114	5010	23612	97962881	-3574	-11627	25	79D	-11635	619
WC151	36	4739	114	4998	23617	97962893	-3549	-11603	24	77D	-11613	630
WC152	36	4727	114	4986	23718	97962830	-3499	-11589	23	76D	-11599	628
WC153	36	4717	114	4973	23570	97962928	-3526	-11565	27	81D	-11571	642
WC154	36	4711	114	4961	23121	97963250	-3618	-11503	24	78D	-11511	689
WC155	36	4704	114	4948	22910	97963382	-3674	-11488	5	59D	-11513	674
WC156	36	4698	114	4936	22880	97963401	-3674	-11478	13	66D	-11496	680

WC157	36	4691	114	4924	22612	97963586	-3731	-11443	26	80D	-11447	717
WC158	36	4684	114	4911	22306	97963795	-3800	-11408	10	67D	-11424	726
WC159	36	4681	114	4899	22160	97963892	-3836	-11394	8	66D	-11410	731
WC160	36	4678	114	4886	22225	97963855	-3807	-11387	4	61D	-11409	721
WC161	36	4674	114	4874	22312	97963826	-3749	-11359	2	58D	-11384	736
WC162	36	4671	114	4861	22309	97963849	-3724	-11333	5	61D	-11355	755
WC163	36	4667	114	4848	22686	97963637	-3576	-11313	22	74D	-11324	775
WC164	36	4663	114	4835	22551	97963795	-3539	-11230	3	56D	-11258	831
WC165	36	4660	114	4821	22377	97964016	-3477	-11109	5	61D	-11131	947
WC166	36	4656	114	4808	22614	97963947	-3318	-11031	1	54D	-11060	1008
WC167	36	4653	114	4795	22504	97964074	-3290	-10965	3	58D	-10991	1070
WC168	36	4650	114	4784	22368	97964204	-3283	-10912	5	63D	-10933	1117
WC169	36	4643	114	4772	22550	97964119	-3187	-10878	10	63D	-10898	1139
WC170	36	4637	114	4771	22711	97964160	-2986	-10732	6	56D	-10760	1271
WC171	36	4630	114	4762	22487	97964190	-3157	-10826	30	82D	-10828	1194
WC172	36	4621	114	4751	22375	97964324	-3115	-10746	12	64D	-10765	1245
WC173	36	4613	114	4740	22437	97964367	-3002	-10655	18	68D	-10670	1327
WC174	36	4604	114	4729	22672	97964211	-2924	-10657	4	49D	-10691	1294
WC175	36	4596	114	4718	22635	97964167	-2991	-10711	4	48D	-10747	1227
WC176	36	4590	114	4706	22294	97964379	-3091	-10695	12	60D	-10717	1246
WC177	36	4586	114	4694	22159	97964470	-3122	-10679	17	68D	-10694	1259
WC178	36	4582	114	4682	22236	97964460	-3053	-10637	26	75D	-10645	1297
WC179	36	4589	114	4681	22879	97964129	-2790	-10593	67	109D	-10568	1378
WC180	36	4592	114	4686	22704	97964235	-2853	-10596	63	107D	-10573	1379
WC181	36	4613	114	4724	23113	97963984	-2749	-10632	16	60D	-10658	1330
WC183	36	4477	114	4807	20287	97965449	-3745	-10665	65	147D	-10594	1351
WC184	36	4482	114	4809	20476	97965367	-3657	-10641	53	130D	-10588	1361
WC185	36	4475	114	4825	20249	97965506	-3721	-10627	53	133D	-10570	1385
WC186	36	4478	114	4837	20828	97965404	-3283	-10387	37	104D	-10361	1603
WC187	36	4483	114	4851	20419	97965306	-3773	-10737	33	110D	-10704	1273
WC188	36	4487	114	4857	20093	97965221	-4170	-11023	38	124D	-10975	1009
WC189	36	4498	114	4868	20114	97965177	-4210	-11071	25	111D	-11035	962
WC190	36	4511	114	4875	20118	97965128	-4274	-11136	60	146D	-11066	946
WC191	36	4518	114	4885	20136	97965078	-4318	-11185	41	127D	-11134	888
WC192	36	4523	114	4897	20178	97965002	-4361	-11243	72	159D	-11161	872
WC193	36	4523	114	4912	20244	97964925	-4376	-11281	67	155D	-11202	842
WC194	36	4526	114	4926	20329	97964861	-4365	-11298	33	122D	-11253	802
WC195	36	4529	114	4939	20390	97964805	-4368	-11322	11	102D	-11297	767
WC196	36	4533	114	4951	20375	97964806	-4387	-11336	13	107D	-11306	768
WC197	36	4537	114	4964	20357	97964805	-4410	-11353	31	129D	-11301	785
WC198	36	4541	114	4977	20385	97964786	-4409	-11361	37	137D	-11301	797
WC199	36	4545	114	4989	20422	97964718	-4448	-11413	30	131D	-11359	748
WC200	36	4549	114	5002	20469	97964594	-4533	-11514	6	108D	-11483	634
WC201	36	4553	114	5014	20477	97964489	-4637	-11620	25	130D	-11568	559
WC202	36	4560	114	5025	20544	97964370	-4703	-11709	4	108D	-11679	461
WC203	36	4566	114	5036	20557	97964266	-4803	-11814	27	133D	-11759	392
WC204	36	4570	114	5049	20619	97964168	-4849	-11881	2	109D	-11849	312
WC205	36	4574	114	5062	20621	97964127	-4893	-11926	2	112D	-11892	281
WC206	36	4578	114	5074	20645	97964103	-4901	-11942	2	114D	-11905	280
WC207	36	4581	114	5087	20679	97964094	-4882	-11935	2	117D	-11896	300
WC208	36	4585	114	5099	20723	97964105	-4835	-11903	5	123D	-11859	348
WC209	36	4589	114	5112	20836	97964082	-4758	-11864	18	135D	-11807	411
WC210	36	4592	114	5125	20941	97964079	-4667	-11809	2	120D	-11767	462
WC211	36	4597	114	5137	20953	97964077	-4664	-11811	1	123D	-11767	471
WC212	36	4601	114	5149	21001	97964056	-4646	-11809	1	126D	-11762	487
WC213	36	4605	114	5162	21047	97964034	-4631	-11809	0	129D	-11759	501
WC214	36	4608	114	5175	20979	97964054	-4679	-11834	1	140D	-11772	499

WC215	36	4612	114	5187	20953	97964080	-4683	-11829	1	149D	-11760	523
WC216	36	4616	114	5201	20965	97964080	-4678	-11828	2	160D	-11747	547
WC217	36	4624	114	5211	21032	97964045	-4661	-11834	1	158D	-11755	551
WC218	36	4628	114	5223	21066	97964060	-4620	-11805	3	168D	-11715	601
WC219	36	4629	114	5236	21184	97964049	-4521	-11747	27	204D	-11622	704
WC220	36	4626	114	5252	21271	97964092	-4392	-11647	100	303D	-11424	911
WC221	36	4629	114	5252	21312	97964085	-4365	-11634	80	275D	-11439	898
WC222	36	5736	114	5534	26299	97960382	-4980	-13949	0	62D	-13982	-735
WC223	36	5747	114	5558	26342	97960444	-4893	-13878	1	62D	-13910	-643
WC224	36	5753	114	5570	26459	97960410	-4826	-13850	1	62D	-13883	-607
WC225	36	5758	114	5581	26389	97960509	-4800	-13800	1	63D	-13832	-550
WC226	36	5763	114	5593	26245	97960664	-4788	-13739	2	64D	-13769	-478
WC227	36	5769	114	5604	26125	97960791	-4782	-13692	1	64D	-13722	-421
WC228	36	5774	114	5616	26046	97960899	-4756	-13639	1	65D	-13667	-355
WC229	36	5780	114	5628	26042	97960943	-4724	-13606	1	66D	-13634	-314
WC230	36	5786	114	5639	26195	97960868	-4664	-13598	1	65D	-13627	-297